New Insights into the Structure and Properties of Electroactive Polymer Films Derived from [Ni(salen)]

Miguel Vilas-Boas,[†] Cristina Freire,*[,†] Baltazar de Castro,[†] Paul A. Christensen,[‡] and A. Robert Hillman[§]

CEQUP/Departamento de Química, Faculdade de Ciências, Universidade do Porto, 4150 Porto, Portugal, Chemistry Department, The University of Newcastle, Newcastle upon Tyne NE1 7RU, U.K., and Department of Chemistry, University of Leicester, Leicester LE1 7RH, U.K.

Received April 25, 1997[⊗]

Oxidative electrochemical polymerization of (*N*,*N*′-ethylenebis(salicylideneaminato)) nickel(II), [Ni(salen)], in acetonitrile/TEAP was reinvestigated. The polymers were characterized by *in situ* FTIR and UV−visible spectroscopies in order to explore film structure and to clarify the electronic states as a function of the electrochemically controlled applied redox potential; oxidized species involved in polymerization and oxidative switching of the polymer were also assessed by *ex situ* EPR experiments. Integration of data from all techniques revealed that (a) electropolymerization of [Ni(salen)] is ultimately a ligand-based-process that takes place through a mixture of *o*- and *p*-linking of the phenyl rings and (b) poly[Ni(salen)] exhibits physical/chemical properties that cannot be attributed to an aggregation of individual complexes, behaving rather like a polyphenylene compound, with the metal ion acting as a bridge between biphenylene moieties.

Introduction

Nickel(II) complexes with tetradentate N_2O_2 Schiff base ligands derived from salicylaldehydes and aliphatic diamines are reversibly reduced to Ni(I) species in several solvents and have been used as homogeneous electrocatalysts in the reduction of alkyl and aryl halides.[1−3] However the oxidative chemistry of these nickel(II) complexes is more intricate: they are oxidized to six-coordinate Ni(III) complexes in strong donating solvents (*N*,*N*′-dimethylformamide and dimethyl sulfoxide), as has been clearly demonstrated by the conjugation of electrochemical techniques and EPR,[4−7] whereas in moderately/weak donor solvents (acetonitrile and solvents with lower DN values) they are oxidatively polymerized at the electrode surfaces to generate electroactive films.[8−18] These nickel-modified electrodes may be used as heterogeneous catalysts in redox reactions, but structural characterization and electrochemical responses/charge storage mechanisms of the transition metal-based polymers play a key step in defining their catalytic activity.

The oxidative polymerization of Ni(II) tetradentate Schiff base complexes has been studied by several groups. It was first reported by Goldsby and co-workers,[8−10] who electropolymerized several nickel complexes with salen and derivatives on platinum- and indium-doped tin oxide-coated glass electrodes and characterized the resulting polymers by cyclic voltammetry, electronic spectroscopy, and scanning electron microscopy. Devynck[11] studied the polymerization of nickel(II) complexes on glassy carbon electrodes and the redox-switching process by electrochemical techniques. Audebert and collaborators[12−15] electrosynthesized nickel and copper polymers based on Schiff base ligands and performed electrochemical, structural, and *in situ* electronic spectroscopic studies. More recently Dahm and co-workers[16−18] reinvestigated the polymerization and the anodically formed nickel salen polymer films on glassy carbon, optically transparent tin oxide, and platinum electrodes using cyclic voltammetry along with spectroelectrochemistry and scanning electron microscopy.

Goldsby[8,9] observed that polymer formation was inhibited by methyl groups bound in the *para* positions of phenol moieties and suggested that polymerization took place by formation of C−C bonds in the *para* positions of the aldehyde moieties between two monomers. These results were corroborated by the structural characterization of the polymers performed by Audebert,[12] based on analysis of the products resulting from cleavage of polymers in concentrated aqueous hydrochloric acid. Nevertheless, the mechanism of the polymerization and the oxidative electrochemical behavior of the polymer are not fully understood and are a matter of current debate. Goldsby[10] and Audebert[12−14] have proposed that the oxidative polymerization of nickel is ultimately a ligand-based-process in which a radical−radical coupling mechanism is responsible for polymer

[†] Universidade do Porto.
[‡] The University of Newcastle.
[§] University of Leicester.
[⊗] Abstract published in *Advance ACS Abstracts,* September 15, 1997.

(1) Gosden, C.; Healy, K. P.; Pletcher, D. *J. Chem. Soc., Dalton Trans.* **1978**, 972.
(2) Healy, K. P.; Pletcher, D. *J. Organomet. Chem.* **1980**, *186*, 401.
(3) Gosden, C.; Kerr, J. B.; Pletcher, D.; Rosas, R. *J. Electroanal. Chem. Interfacial Electrochem.* **1981**, *117*, 101.
(4) Castro, B.; Freire, C. *Inorg. Chem.* **1990**, *29*, 5113.
(5) Carrondo, M. A. A. F. C. T.; Castro, B; Coelho, A. M.; Domingues, D.; Freire, C.; Morais, J. *Inorg. Chim. Acta* **1993**, *205*, 157.
(6) Azevedo, F.; Carrondo, M. A. A. F. C. T.; Castro, B; Convery, M.; Domingues, D.; Freire, C.; Duarte, M. T.; Nielsen, K.; Santos, I. C. *Inorg. Chim. Acta* **1994**, *219*, 43.
(7) Castro, B.; Freire, C. Submitted for publication.
(8) Goldsby, K. A. *J. Coord. Chem.* **1988**, *19*, 83
(9) Goldsby, K. A.; Blaho, J. K.; Hoferkamp, L. A. *Polyhedron* **1989**, *8*, 113.
(10) Goldsby, K. A.; Hoferkamp, L. A. *Chem. Mater.* **1989**, *1*, 348.
(11) Bedioui, F.; Labbe, E.; Gutierrez-Granados, S.; Devynck, J. *J. Electroanal. Chem. Interfacial Electrochem.* **1991**, *301*, 267.
(12) Audebert, P.; Capdevielle, P.; Maumy, M. *New J. Chem.* **1991**, *15*, 235.
(13) Audebert, P.; Capdevielle, P.; Maumy, M. *Synth. Met.* **1991**, *41*, 3049.
(14) Audebert, P.; Capdevielle, P.; Maumy, M. *New J. Chem.* **1992**, *16*, 697.
(15) Audebert, P.; Hapiot, P.; Capdevielle, P.; Maumy, M. *J. Electroanal. Chem. Interfacial Electrochem.* **1992**, *338*, 269.
(16) Dahm, C. E.; Peters, D. G. *Anal. Chem.* **1994**, *66*, 3117.
(17) Dahm, C. E.; Peters, D. G. *J. Electroanal. Chem. Interfacial Electrochem.* **1996**, *406*, 119.
(18) Dahm, C. E.; Peters, D. G. *J. Electroanal. Chem. Interfacial Electrochem.* **1996**, *410*, 163.

S0020-1669(97)00467-9 CCC: $14.00

formation. In his recent paper, Dahm[18] proposes a metal-centered oxidation process followed by irreversible formation of phenyl−phenyl linkages between different Ni(III) species. Regarding the oxidative electrochemical behavior of the polymer, Dahm also considered it to be metal centered, whereas Audebert, noting that changing the metal ion (Cu *vs* Ni) appears to have little effect on conductivity and that some polymers were conducting in the dry state (implying some delocalization of the positive charges along the aromatic ligand system), proposed that it should be associated with a ligand centered process of the surface redox couple.[14,15]

To distinguish between the two proposed behaviors for poly[Ni(salen)], the use of spectroscopic studies is required. In this paper, we use *in situ* spectroscopic methods (UV−vis and FTIR) to explore film structure and electronic properties as a function of electrochemically controlled redox applied potential. FTIR spectroscopy directly probes the polymerization mechanism and the path of electronic conduction, whereas UV−vis spectroscopy provides insights into the electronic states of the polymer. The oxidized species involved in polymerization and in the oxidative switching of the polymer are also assessed by qualitative *ex situ* EPR experiments.

Experimental Section

Instrumentation. (a) Electrochemistry. Electrochemical measurements were performed using an EG&G PAR 273A potentiostat/galvanostat, with a standard three-electrode cell: cyclic voltammetry was performed using a Pt disk electrode with an area of 0.0314 cm^2 and a Pt gauze as the counter electrode; all the potentials refer to an Ag/AgCl (0.1 mol dm^{-3} NaCl) reference electrode. Prior to use, the working electrode was polished with an aqueous suspension of 0.05 μm alumina (Beuhler) on a Master-Tex (Beuhler) polishing pad. Solutions were deareated by passing a current of argon prior to each experiment, which was run also under an argon atmosphere.

(b) IR Spectroscopy. The FTIR spectrometer employed was a Bio-Rad FTS-60. The spectra were obtained at 8 cm^{-1} resolution and comprised 100 co-added and averaged scans. The detector speed employed was 40 kHz. The FTIR spectrometer was controlled by an Oxsys Micros Electrochemical Interface, which also controlled the electrochemistry in the spectroelectrochemical cell. The spectroelectrochemical cell was a standard three-electrode, thin-layer design, which is described in detail elsewhere.[19,20] The window employed was a 2.5 cm diameter × 0.3 cm thick CaF_2 plate. The counter electrode was a Pt wire loop, and the reference electrode was a commercial (S. H. Scientific) Ag/AgCl electrode, separated from the cell itself by a salt bridge containing 0.1 mol dm^{-3} TEAP, to minimize contamination by water. The working electrode was a solid "top hat"-shaped piece of Pt. In the spectra given, a reference spectrum S_r, was collected at a reference potential, E_r. The potential was then stepped down or up in 0.1 V increments, and spectra S_n were taken at each potential E_n. The spectra are represented as a normalized difference $\Delta R/R$: $\Delta R/R = (S_n - S_r)/S_r$.

(c) UV−Visible Transmission Spectroscopy. The spectroscopic instrumentation used, based on a Hewlett Packard HP8451A spectrophotometer, was described elsewhere.[21] Spectroscopic measurements were made *in situ* in the transmission mode, with the electrode under potential control, using a home made potentiostat. The electrode was an indium tin oxide-coated conducting glass (ITO, Balzers) and its area (typically 2.1 cm^2) was defined by a silicone sealant (Dow Corning 3145RTV). All potentials were measured and quoted with respect to an Ag/AgCl (NaCl 0.1 mol dm^{-3}) reference electrode; the counter electrode was a Pt gauze. The spectrometer was programmed to acquire spectra at 10 s intervals in the range 300−820 nm. A background spectrum (0.1 mol dm^{-3} TEAP/CH_3CN) and a reference spectrum (1 mmol dm^{-3} [Ni(salen)] in 0.1 mol dm^{-3} TEAP/CH_3CN) were collected before the modification of the electrode.

(d) Electron Paramagnetic Resonance Spectroscopy. EPR spectra were obtained with an X-band Bruker ESP 300E spectrometer, both at room temperature and at 77 K. Spectra were calibrated with diphenylpicrylhydrazyl (dpph; $g = 2.0037$), and the magnetic field was calibrated by use of Mn(II) in MgO. The samples were prepared as poly[Ni(salen)] modified Pt wires, ($\Phi = 0.025$ cm), that were then inserted into quartz EPR tubes ($\Phi = 0.4$ cm).

Materials. [Ni(salen)], (*N,N′*-ethylenebis(salicylideneaminato))-nickel(II), was prepared by a procedure described in the literature[22] and recrystallized from acetonitrile. Tetraethylammonium perchlorate (TEAP) was prepared from tetraethylammonium bromide (Aldrich) and perchloric acid (Merck, p.a.) and purified by recrystallization from water.[23] Acetonitrile (Fisions, HPLC grade) was refluxed over CaH_2 and distilled under Ar or N_2 before use.

Procedures. Poly[Ni(salen)] films were deposited by cycling the potential of the working electrode either between 0 and 1.6 V or between 0 and 1.3 V; scan rates were 0.005 V s^{-1} for UV−vis, 0.010 V s^{-1} for electrochemical measurements, and 0.006 V s^{-1} for FTIR studies. Solutions containing 1 mmol dm^{-3} [Ni(salen)] in 0.1 mol dm^{-3} TEAP/CH_3CN were used. For quantitative experiments, the films were prepared using a single voltammetric cycle.

After the electropolymerization, the modified electrode was rinsed with dry CH_3CN and the experiments were carried out on films immersed in 0.1 mol dm^{-3} TEAP/CH_3CN; the modified electrode was cycled from 0.0 to 1.6 V or from 0.0 to 1.0 V. Coulometric assay in monomer-free solution indicated polymer film coverages equivalent to *ca.* 110 nmol cm^{-2} of electroactive sites.

Poly[Ni(salen)] films in the neutral state for EPR experiments were obtained by cycling the potential at 0.010 V s^{-1} (10 cycles) in 1 mmol dm^{-3} [Ni(salen)] in 0.1 mol dm^{-3} TEAP/CH_3CN, by using the potential ranges referred above, but with the end of the cycle at 0 V. Films in the oxidized state were prepared by controlled-potential oxidation (5 and 10 min) at either 1.0, 1.3, or 1.6 V *vs* Ag/AgCl (NaCl 0.1 mol dm^{-3}). After preparation, the modified Pt wire with the film was washed thoroughly with dry CH_3CN, dried in a argon stream, and inserted into an EPR tube that was immediately sealed.

Results and Discussion

Electrochemistry. Figure 1a depicts the results of an exploratory cyclic voltammetric experiment used to polymerize [Ni(salen)] from solution and to produce a surface-immobilized poly[Ni(salen)] film. The experiment consists of a series of slow scan rate (0.010 V s^{-1}) excursions to positive potentials. [Ni(salen)] oxidation occurs at potentials above *ca*. 0.80 V and is associated with an anodic current peak at 1.04 V, with a shoulder at 0.98 V. Upon scan reversal at 1.60 V, there is a single cathodic peak at 0.77 V. Qualitative inspection of the anodic and cathodic charges passed in the first potential cycle of this experiment clearly indicates an irreversible process. Visual inspection of the electrode also shows the deposition of a green film (see visible transmission spectra, below), the thickness of which increases upon successive potential cycles. This film is not dissolved upon subsequent anodic or cathodic potential sweeps; *i.e.*, it is not simply the result of precipitation of an insoluble monomeric Ni(salen)-based complex. In accord with the work of Goldsby,[9,10] Audebert,[12−15] and Dahm,[18] we conclude that the product of [Ni(salen)] oxidation is a polymeric material, whose structure and properties we now explore using spectroscopic methods.

(19) Christensen, P. A.; Hamnett, A.; Hillman, A. R.; Swann, M. J.; Higgins, S. J. *Synth. Met.* **1994**, *62*, 14.
(20) Christensen, P. A.; Hamnett, A.; Read, D. C. *Electrochim. Acta* **1994**, *39*, 187.
(21) Hillman, A. R.; Mallen, E. F. *J. Electroanal. Chem. Interfacial Electrochem.* **1988**, *224*, 403.
(22) Holm, R. H.; Everett, G. W., Jr.; Chakravorty, A. *Prog. Inorg. Chem.* **1966**, *7*, 183.
(23) Donald, S. T., Jr.; Julien, R. L. *Experimental Electrochemistry for Chemistry*; Wiley: New York, 1974.

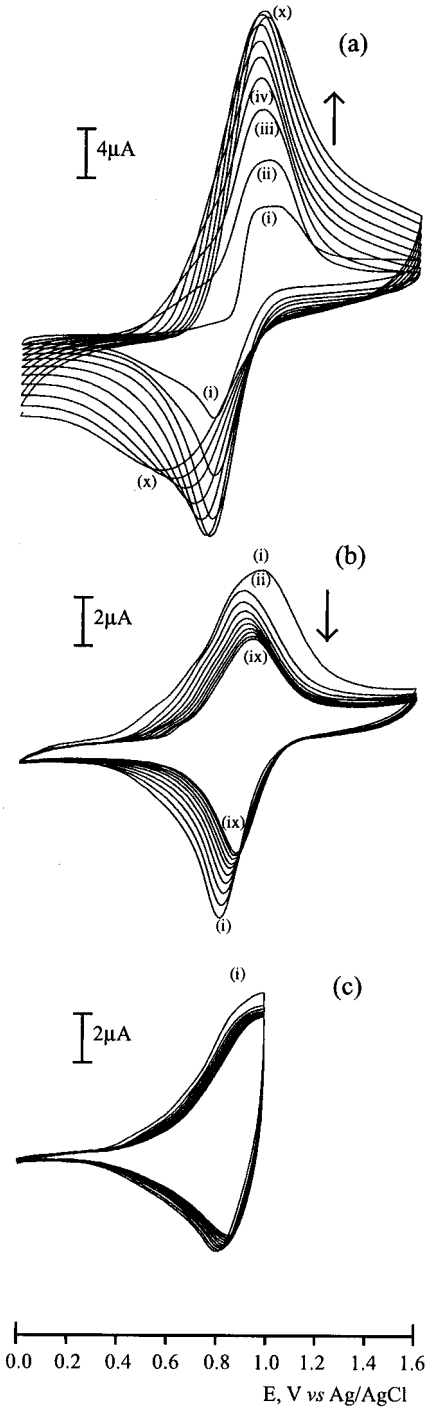

Figure 1. (a) Cyclic voltammogram showing the anodic polymerization of 1 mmol dm^{-3} [Ni(salen)] in 0.1 mol dm^{-3} TEAP/CH_3CN at a platinum disk electrode, between 0 and 1.6 V at 0.0010 V s^{-1}: (i) first cycle, ..., and (x) tenth cycle. (b) Cyclic voltammogram of a poly-[Ni(salen)]-modified electrode in 0.1 mol dm^{-3} TEAP/CH_3CN between 0 and 1.6 V at 0.0010 V s^{-1}: (i) first cycle, ..., and (ix) ninth cycle. (c) Cyclic voltammogram of a poly[Ni(salen)]-modified electrode in 0.1 mol dm^{-3} TEAP/CH_3CN, between 0 and 1.0 V at 0.0010 V s^{-1}: (i) first cycle.

Figure 1a also shows that the current responses to subsequent potential cycles decrease progressively after nine cycles. On the basis of this experiment alone, one cannot determine whether this is associated with film deterioration (overoxidation) at the rather positive potential limit employed or whether the film is electroactive and either impedes the oxidation of additional monomer in solution or is exposed to a depleted reservoir of reactant monomer in the diffusion layer adjacent to the electrode. This issue is resolved by the experiment of Figure 1b, in which the solution has been replaced by monomer-free electrolyte, so that any current response must be solely attributable to a surface-bound film.

In Figure 1b, we see electrochemical responses attributable to redox conversion of the film. The first scan is different from the subsequent scans: it has two anodic waves at potentials very similar to those of the polymerization and one cathodic wave; subsequent scans exhibit only one anodic wave that is shifted positively (0.040 V) and a single cathodic wave (at 0.81 V), attributable to redox conversion of the film. The magnitudes of the current peaks decrease with progressive redox cycling. We therefore conclude that we have been successful in immobilizing an electroactive polymer but that its stability is limited. In comparison, Figure 1c shows the analogous experiment, but for a film deposited and subsequently redox-cycled using anodic potential limits of 1.3 and 1.0 V, respectively (*cf.* Figure 1a,b). Now, the same general features are observed, but with increased stability. A series of experiments employing different anodic potential limits showed that polymerization potentials below *ca.* 1.0 V did not produce films of sufficient thickness or stability for characterization. Unless otherwise specified, all subsequent experiments therefore employed polymerization and redox-cycling protocols with anodic potential limits in the range 1.0−1.3 V, as indicated in the figure captions.

We now consider the coulometry of the system under these more moderate conditions, *i.e.* when the charge associated with film degradation is small. We therefore have to consider three possible processes contributing to the overall charge passed: polymerization, ligand-based redox processes, and metal-based redox processes. Polymerization by coupling of the phenyl rings will be associated with removal of one electron and one proton from each phenyl ring, *i.e.* two electrons per monomer unit. In the reversible redox switching of the polymer (second scan), let the extent of phenyl ring oxidation ("doping level") be y electrons per ring, *i.e.* $2y$ electrons per monomer unit, and the extent of Ni(II/III) redox switching be z electrons per metal site, where $z = 0$ or 1. Now the ratio of anodic charges passed in the polymerization/deposition and subsequent voltammetry experiment (analogous to Figure 1a and Figure 1b, respectively) is $Q_{pol}/Q_{redox} = (2 + 2y + z)/(2y + z)$. Experimentally, we find this ratio to be 4.27, from which $(2y + z) = 0.62$; *i.e.*, $z = 0$ and $y = 0.31$. This corresponds to a ligand-based, rather than a metal-based, redox process, in accord with the conclusions of Goldsby[8−10] *et al.* and Audebert *et al.*[12−15] In our case, we can go further and say that, at the positive potential limit employed, two positive charges are delocalized across approximately six phenyl rings, *i.e.* three monomer units. The above coulometric data provide a means to distinguish indirectly between metal-based (Ni(II/III)) and ligand-based processes. We now address this issue more directly on the basis of the associated spectroscopic responses.

***In Situ* FTIR Experiments. (a) Overview.** *In situ* FTIR spectra over the range 1000−1700 cm^{-1} obtained from the bare Pt electrode immersed in 1 mmol dm^{-3} [Ni(salen)]/0.1 mol dm^{-3} TEAP/CH_3CN solution and a polymer-coated electrode immersed in 0.1 mol dm^{-3} TEAP/CH_3CN at 0.0 V are shown in Figure 2 (with the voltammogram inset). The primary features in vibrational region of the FTIR spectra are summarized in Table S1, Supporting Information. As can be seen, the monomer and polymer spectra are broadly similar in all but the spectral region between 1360 and 1560 cm^{-1}, with a number of new bands (1377, 1396, 1407, 1423, 1450, 1461, 1481, 1495, and 1515 cm^{-1}) appearing on polymerization and the broad, strong monomer absorption near 1454 cm^{-1} being lost.

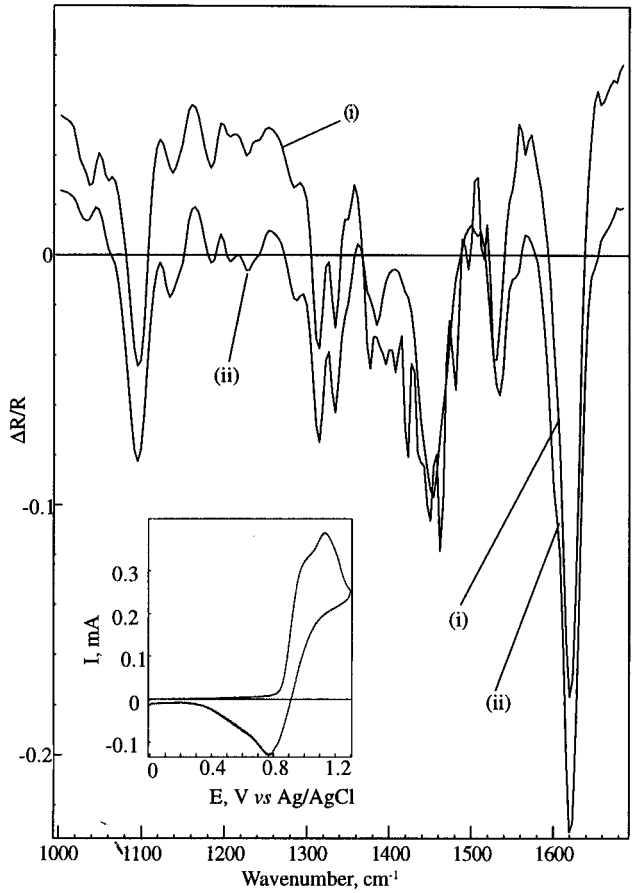

Figure 2. *In situ* FTIR reflectance spectra of (i) a poly[Ni(salen)]-coated electrode in 0.1 mol dm^{-3} TEAP/CH_3CN, obtained by anodic polymerization of 1 mmol dm^{-3} [Ni(salen)] in 0.1 mol dm^{-3} TEAP/CH_3CN solution, between 0 and 1.3 V at 0.006 V s^{-1} (cyclic voltammogram inset), and (ii) a bare Pt electrode immersed in 1 mmol dm^{-3} [Ni(salen)] in 0.1 mol dm^{-3} TEAP/CH_3CN.

Assignments of vibrational bands are based on previous spectroscopic studies of [Ni(salen)][24] and [(UO_2)(salen)-(solvent)][25,26] complexes. We also build upon studies of polymeric heterocycles, typified by polypyrrole[27] and polythiophenes.[28,29] The key feature is that those modes which involve a substantial change in dipole moment in the direction of charge delocalization produce considerably enhanced bands (termed IRAV bands) in the IR spectrum. As discussed previously,[27−29] this is a consequence of the facile movement of electronic charge along the polymer chain and the interaction of these mobile charge carriers with the dipole moment.

Panels a and b of Figure 3 show absolute reflectance spectra (*i.e.* normalized to the bare Pt electrode) of the polymer film in Figure 2 taken at 0.1 V intervals from 0.3 to 1.0 V. Figure 3a shows the full spectral range from 700 to 6600 cm^{-1}, and Figure 3b, the region from 700 to 1800 cm^{-1}. Figure 3a is dominated by a broad, intense band which extends from 1700 cm^{-1} out into the near-IR and appears to have a maximum near 5200 cm^{-1}. The maximum is difficult to locate accurately because

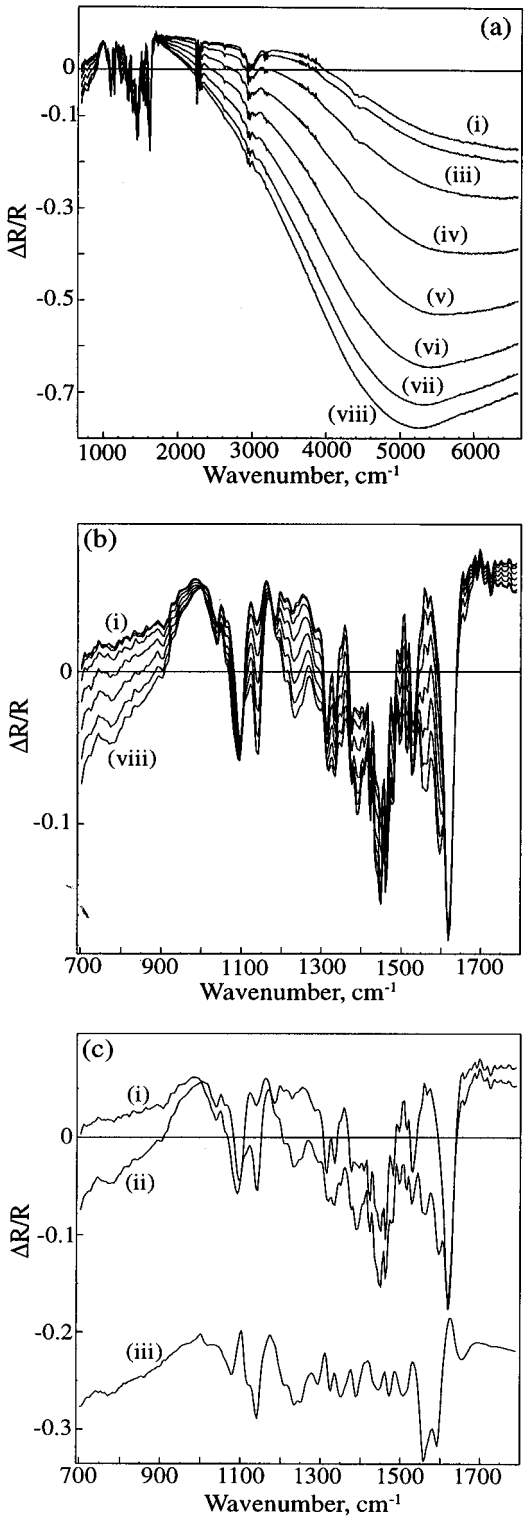

Figure 3. *In situ* FTIR reflectance spectra of a poly[Ni(salen)]-coated electrode in 0.1 mol dm^{-3} TEAP/CH_3CN taken at 0.1 V intervals from 0.3 to 1.0 V: (a) full spectral range, 700−6600 cm^{-1}, from 0.3 V (i) to 1.0 V (viii); (b) 700−1800 cm^{-1}, from 0.3 V (i) to 1.0 V (viii); (c) 700−1800 cm^{-1}, at (i) 0.3 V and (ii) 1.0 V, also showing (iii) the difference spectrum.

the spectrum of Figure 3a is distorted as a result of small differences in alignment of the electrode between the reference spectrum of the bare electrode and the spectra of the coated Pt. This problem is removed if the spectra are normalized to the first spectrum taken of the coated electrode at 0.3 V[19,20] (Figure S1a, Supporting Information). It can be seen that the maximum in the broad band is actually nearer 4900 cm^{-1}.

(24) Datta, M.; Brown, D. H.; Smith, W. E. *Spectrochim. Acta* **1983**, *39A*, 37.
(25) Almadfa, H.; Said, H. H.; Nour, E. M. *Bull. Soc. Chim. Fr.* **1991**, *128*, 137.
(26) Nour, E. M.; Taha, A. A.; Alnaimi, I. S. *Inorg. Chim. Acta* **1988**, *141*, 139.
(27) Christensen, P. A.; Hamnett, A. *Electrochim. Acta* **1991**, *36*, 1263.
(28) Christensen, P. A.; Hamnett, A.; Hillman, A. R.; Swann, M. J.; Higgins, S. J. *J. Chem. Soc., Faraday Trans.* **1992**, *88*, 595.
(29) Christensen, P. A.; Hamnett, A.; Hillman, A. R.; Swann, M. J.; Higgins, S. J. *J. Chem. Soc., Faraday Trans.* **1993**, *89*, 921.

Table 1. Effect of Film Oxidation on Polymer Vibrational Band Intensities

band/cm^{-1}	enhanced?	comments
800	yes	not present at 0.3 V
1035	no	
1058 (sh)	no	
1096	slightly	moves down to *ca.* 1090 cm^{-1} and broadens[a]
1115 (sh)	yes	not present at 0.3 V
1138	yes	large increase in intensity
1184	no	
1206	yes	
1227	yes	large increase in intensity
1240	yes	large increase in intensity
1284	yes	
1314	no	
1325	yes	not present at 0.3 V
1334	yes	
1350	yes	
1377	no	
1396	yes	
1407	no	
1423	yes	
1438 (sh)	yes	
1450	yes	
1461	no	
1475	yes	not present at 0.3 V
1481	no	
1495	no	
1515	yes	
1528	no	large decrease in intensity
1550	yes	
1601	yes	not present at 0.3 V
1620	no	

[a] Bipolar band.

(b) Vibrational Features. Inspection of the monomer structure suggests four possible polymerization mechanisms: (i) *p*-linking of the phenyl rings (to give a −Ph−Ph−Ni− structure, reminiscent in some respects of polyphenylene), (ii) *o*-linking of the phenyl rings, (iii) formation of ···Ni−Ni··· stacks (perpendicular to the plane of the ligand), and (iv) formation of ···Ni−phenyl··· stacks, to give a staggered structure perpendicular to the plane of the ligand. Figure 3b and Table S1 show features at 1377, 1450, and 1515 cm^{-1} attributable to phenyl ring in-plane vibrations. The IRAV enhancement of these features upon oxidation (Table 1) immediately allows us to discount structures in which charge delocalization is perpendicular to the rings, *i.e.* the "stack" structures of possibilities iii and iv. IRAV bands at 1138, 1227, 1240, and 1284 cm^{-1}, attributed[24,25] to C−C, C−O, or C−N vibrations, are observed. A small, non-IRAV, feature is observed at 1184 cm^{-1}. These modes all involve vibration in the plane of the molecule. The strong IRAV bands are consistent with possibilities i and ii; we return to the lack of enhancement of some of these in-plane modes later.

The spectrum of Figure 2 shows that the polymer absorptions are very similar to those of the monomer;[24] almost all the significant differences are in the region 1360−1500 cm^{-1}, which includes the phenyl ring absorption region.[29,30] The most intense absorption, that near 1620 cm^{-1}, is unchanged on polymerization; this feature may be assigned to the C═N stretch of the salen ligand.[24,25] In addition, the features in the region 1000−1350 cm^{-1}, which would be expected to include the C−O stretch of the salen ligand, are also largely unchanged on polymerization. These observations are all consistent with polymerization through the phenyl rings, as postulated above.

The changes in vibrational bands that we do see for the (neutral) polymer, as compared to the monomer, are primarily in the region 1380−1420 cm^{-1}, where the bands have previously been assigned to various phenyl ring modes.[24] We can therefore be confident that polymerization involves linkage of phenyl rings of neighboring [Ni(salen)] units. On the basis of the present data and the level of interpretation of the monomer spectra in the literature, we cannot however distinguish between *o*- and *p*-linked rings. Simple synthetic methods allow blocking of both the *o*- and *p*-positions with chloride atoms. These derivatives do not polymerize,[10,31] again supporting the idea of phenyl−phenyl linkages. We suggest that there is a mixture of *o*- and *p*-linking, steric effects favoring the latter.

Returning to Figure 3b, it can be seen that a number of the features listed in Table S1 increase in intensity on oxidation of the polymer and some new bands appear. This can be seen more clearly in Table 1 and in Figure 3c, which shows the spectra in Figure 3b taken at 0.3 and 1.0 V. Of particular note are the new bands near 800, 1115, and 1601 cm^{-1}, the bipolar band (in the difference spectrum) centered near 1080 cm^{-1}, the features showing large gains in intensity near 1140, 1206, 1227, 1240, 1396, and 1560 cm^{-1}, and the significant decrease in intensity of the 1528 cm^{-1} band.

It can be seen from Figure 3a that the intensities of the features near 2300 and 3000 cm^{-1}, attributable to the C−N and C−H stretches of acetonitrile,[19,20] decrease as the oxidation proceeds. Figure S1 clearly shows these features as loss bands, and the acetonitrile loss features reveal that the as-grown polymer contains electrolyte. In previous papers on conducting polymers,[19,20] this behavior was interpreted in terms of the "concealing" of electrolyte present in the neutral form of the film on oxidation, due to the increasing reflection of the IR beam from the front face of the polymer. From (a) the intensity of the acetonitrile loss feature near 2625 cm^{-1}, (b) the value of the extinction coefficient of this absorption,[32] $\epsilon \approx 1$ M^{-1} cm^{-1} (assuming it does not change within the film), and (c) the intensity of this feature in the single-beam spectrum of the polymer, it is possible to calculate that the acetonitrile loss corresponds to a concentration of *ca.* 1.1 mol dm^{-3} in the whole of the thin layer; *i.e.*, roughly 6% of the solvent present in the thin layer is present in the film.

(c) Electronic Features of FTIR Spectra. Figures 3a and S1a are dominated by the broad, intense band covering the region *ca.* 2500−6000 cm^{-1}, with a maximum near 4900 cm^{-1}. By analogy with previous work on conducting polymers,[19,20,27] this band may be assigned to an electronic transition resulting from the generation of charge carriers in the polymer on oxidation. On the one hand, the motion of charge carriers associated with this feature is the cause of the IRAV enhancement. On the other hand, as commonly seen for electroactive polyaromatics,[33] this represents the low-energy end of the electronic spectrum, primarily seen in the UV−visible region.

To gain some insight into charge carrier generation, we start by making some straightforward assumptions concerning the relationships between the IRAV and electronic band intensities, ξ_I and ξ_E, respectively. These integrated intensities have been reported to vary linearly with the number of charge carriers, N_c.[34,35] Expressing this in terms of the experimentally accessible

(30) Socrates, G. *Infrared Characteristic Group Frequencies*; Wiley: Bath, England, 1980.

(31) Castro, B.; Freire, C. Work in progress

(32) Christensen, P. A.; Hamnett, A.; Higgins, S. J.; Timney, J. A. *J. Electroanal. Chem. Interfacial Electrochem.* **1995**, *395*, 195.

(33) *Handbook of Conducting Polymers*; Skotheim, T. A., Ed. Marcel Dekker: New York, 1986.

(34) Vardeny, Z.; Tanaka, J.; Fujimoto, H.; Tanaka, M. *Solid State Commun.* **1984**, *50*, 937.

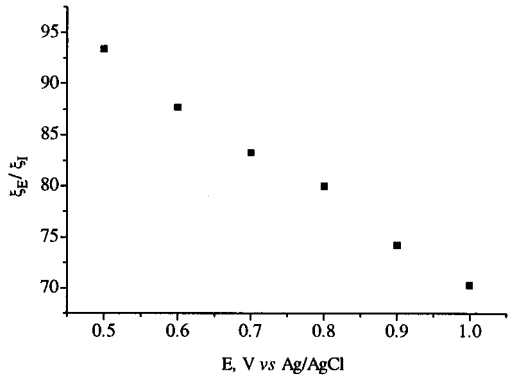

Figure 4. Plot of ξ_E/ξ_I *vs E*, where ξ_I is integrated between 1006 and 1620 cm^{-1}.

quantity charge, Q (which is linearly related to N_c), we have

$$\xi_I = kQ/M_D \quad (1)$$

$$\xi_E = kQ/m_e \quad (2)$$

where ξ_I is integrated between 1006 and 1620 cm^{-1}, k is a constant, M_D is the carrier effective mass, and m_e is the effective electron mass defined in terms of electronic band curvature.[34,35] According to eqs 1 and 2, a plot of ξ_E/ξ_I *vs* Q will reveal any variation in the ratio of the carrier mass to the effective electron mass on polymer oxidation. Data for the film of Figure 2 are presented in Figure 4. For the range of conditions covered ($0.4 < E/V \leq 1.0$) the film shows a nonlinear *decrease* in ξ_E/ξ_I with E, implying that M_D and/or m_e are charge-dependent.

In our previous studies of thiophene-based polymer films,[19,20] we assumed that these variations of carrier mass and electron effective mass with charge were linear:

$$M_D = M_D^0(1 + \kappa_D Q) \quad (3)$$

$$m_e = m_e^0(1 + \kappa_e Q) \quad (4)$$

where κ_D and κ_e are constants. Equations 1−4 yield

$$\xi_E = kQ/m_e^0(1 + \kappa_e Q) \quad (5)$$

$$\xi_I = kQ/M_D^0(1 + \kappa_D Q) \quad (6)$$

Rearranging and combining eqs 5 and 6, we obtain

$$1/\xi_I = (M_D^0/m_e^0)(1/\xi_E) + (M_D^0/k)(\kappa_D - \kappa_e) \quad (7)$$

A plot of $1/\xi_I$ *vs* $1/\xi_E$ should then be linear: the slope will reflect the relative mobility of electrons and positive charge carriers (in the limit of low carrier density), and the intercept will reflect the relative importance of carrier−carrier interactions and mean chain length.

Before applying eq 7 to our data, we note from Figure 3b,c that the vibrational bands in the range 1000−1800 cm^{-1} do not show identical intensity *vs* potential behavior. Pursuing this further, we analyzed the normalized spectra of Figure S1a in segments, which roughly define the various loss and gain features, namely 1000−1094, 1110−1172, 1173−1277, 1278−1311, 1312−1337, 1338−1375, 1376−1412, 1413−1461, 1462−1489, 1490−1530, 1531−1581, and 1582−1615 cm^{-1}. The integrated intensities (individually normalized to their maximum value) of the bands in these regions were plotted as functions of potential. Plots for the regions 1000−1094 and 1278−1311 cm^{-1} are shown in Figure 5; they represent the two types of behavior observed. This distinction is highlighted by the application of eq 7 to these individual regions: plots of $1/\xi_I$ *vs* $1/\xi_E$ for these two representative regions are shown in Figure 6. We ascribe this behavior to the coexistence of (at least) two carrier types, denoted carrier I and carrier II (see Table 2). Carrier I, represented by absorption in the region 1000−1094 cm^{-1}, shows a linear relationship between $1/\xi_I$ and $1/\xi_E$ (Figure 6a), while the corresponding plot for absorptions associated with carrier II (Figure 6b) shows two intersecting lines of different slopes. The successful application of this type of analysis underscores the notion that poly[Ni(salen)] behaves as a delocalized system, rather than a collection of discrete nickel redox centers.

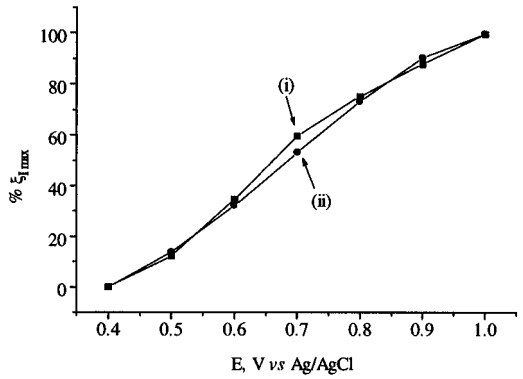

Figure 5. Plot of the integrated IRAV intensity normalized to its maximum value (% $\xi_{I\,max}$) *vs E*, for two different vibrational regions: (i) 1000−1094 cm^{-1}; (ii) 1278−1311 cm^{-1}.

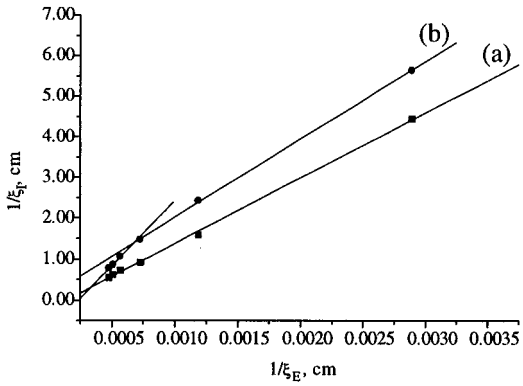

Figure 6. Plot of $1/\xi_I$ *vs* $1/\xi_E$: (a) absorptions in the region 1000−1094 cm^{-1}; (b) absorptions in the region 1278−1311 cm^{-1}.

Table 2. Association of Spectral Regions (cm^{-1}) with Charge Carrier Types

carrier I	carrier II
1000−1094	1110−1172
1312−1337	1173−1277
1376−1412	1278−1311
1413−1461	1338−1375

(d) Redox State Changes and Charge Conduction. Oxidation of the polymer results in selective enhancement of bands associated with some ligand vibrations, as discussed with reference to Figure 3b,c. This is a common observation in the literature of conducting polymers based on aromatic monomers.[19,20,27,36] While not all the bands observed for the neutral form of the polymer are enhanced by oxidation (Table 1), enhancement is observed across the full spectral range from

(35) Pal, A. J.; Ruani, G.; Zamboni, R.; Danieli, R.; Taliani, C. *Synth. Met.* **1991**, *41*−*43*, 579.

(36) Vardeny, Z.; Ehrenfreund, E.; Brafman, O.; Nowak, M.; Schaffer, H.; Heeger, A. J.; Wudl, F. *Phys. Rev. Lett.* **1986**, *56*, 671.

1000 to 1600 cm^{-1}, suggesting that charge transport, at least on the IR time scale, does **not** occur *via* interchain hopping between stacked [Ni(salen)] moieties perpendicular to the chains. If it did, the in-plane ring vibrations expected between 1300 and 1600 cm^{-1} would not be enhanced.

The electronic spectra (see below) also suggest that film electroactivity is ligand- rather than metal-based. Nevertheless, extended delocalization must involve the Ni atom as a bridge between biphenyl units. There are two possible routes for delocalization: through the oxygen or through the nitrogen. The data of Figure 4b,c show a strong band at 1620 cm^{-1}, which we assign[24] to the C═N stretch. Variation of the applied potential, and thus the number and mobility of charge carriers in the delocalized system, does not significantly alter the intensity of this band. We therefore deduce that the C═N moiety is not in the conduction path. The alternative, conduction through the oxygen, might be expected to result in significant intensity variation for the C−O stretch. This is less straightforward to confirm or disprove, since C−C, C−O, and C−N single-bond stretching modes give rise to features in the range 1100−1320 cm^{-1}, where the assignments are somewhat ambiguous.[25] Of the bands we do see in this region (1138, 1206, 1227, and 1240 cm^{-1}), those at 1138 cm^{-1} and, to a lesser extent, at 1227 and 1240 cm^{-1} are significantly enhanced upon polymer oxidation (see Figure S1b). Although not unequivocal, these observations are all consistent with the notion of a $\cdots(-Ph-O-Ni-O-Ph-)_n\cdots$ conduction path.

This model is reminiscent in some respects of a polyphenylene structure. In that system, and in polyheteroaromatics such as polypyrrole and polythiophene, charge delocalization implies the contribution of at least some quinoid structure, *i.e.* partial double-bond character between the aromatic rings of adjacent monomer units. Of necessity, the phenyl−phenyl linkage is in the charge conduction path, so vibrational modes involving this C═C entity should be strongly enhanced. Indeed, upon oxidation of the polymer (see Figure S1b), we see the progressive appearance (from almost zero intensity for the neutral polymer) of bands at 1550 and 1601 cm^{-1}. Although both of these are within the range for vibration of a C−C bond with appreciable double-bond character, the appearance of a shoulder around 1560 cm^{-1} for the monomer (see Figure 2) leads us to propose the 1601 cm^{-1} band as a candidate for the quinoid C═C stretch, which would necessarily be absent in the neutral form. One implication of this interpretation is that the C−O bond might develop some double-bond character or show a significant variation in intensity. Of the bands in the relevant region, those at 1184 and 1207 cm^{-1} are weak and relatively independent of polymer oxidation state; hence, we attribute them to C−C and C−N stretching modes. The bands at 1138, 1227, and 1240 cm^{-1} do not move significantly with polymer oxidation state changes but do increase markedly in intensity upon oxidation; we suggest that at least one of these is associated with a C−O stretch mode. The absence of any significant shift in band position presumably indicates that the positive charge is primarily centered on the phenyl ring. In support of our approach, we cite the work of Pham *et al*. on the infrared spectra of polymers derived from 1-naphthol.[37] They assigned a band at 1552 cm^{-1} to a C−C stretch between phenyl rings in a quinoid structure and a band in the range 1211−1227 cm^{-1} to a stretching mode for a C−O moiety with partial double bond character.

As was stated above, the most intense band in the spectrum of the neutral form at 0.3 V, the C═N stretch near 1620 cm^{-1}, is unchanged on oxidation, (see Figure 3b,c), as is the feature near 1184 cm^{-1}. Clearly, the part of the ligand associated with these vibrations is not influenced at all by the oxidation process, suggesting that the 1184 cm^{-1} absorption is also due to a vibration associated with this fragment, *i.e*. the C−N stretch of the C−N═C moiety. This strongly supports the notion that the C−N═C moiety is not involved in charge propagation. Moreover, the oxidation process cannot involve the oxidation of the central nickel ion, as such a process would be expected to cause a shift in the C═N stretching frequency at the very least. For example, the oxidation of Fe(II) to Fe(III) in the Fe(II)−C≡N$\cdots$ Fe^{2+} moiety of Prussian blue was found[38] to increase the C≡N stretching frequency by 20−30 cm^{-1}.

One alternative conduction path is simply through the phenyl rings, bypassing the C−O and C−N═C linkages altogether. If this was indeed the case, it would be expected that the IR spectra observed during the oxidation of the film should bear some resemblance to those obtained during the oxidation of poly(*p*-phenylene); this is not observed.[37,39−41] In any case such a process would be sterically inhibited.

Pham *et al.*[42,43] studied poly(1-naphthol) using multiple internal reflection FTIR spectroscopy (MIRFTIRS). They observed a band near 1223 cm^{-1} that appears and increases in intensity on oxidation of the polymer. This band was assigned to the C−O−C moiety with a positive charge on the O (or delocalized between all three). In the absence of any real alternatives, it does not seem unreasonable to postulate that the feature near 1140 cm^{-1} (see Figure 3b,c), which is one of the most significantly enhanced bands, is due to an analogous moiety, C−O−Ni. In addition, there is a band appearing alongside the feature near 1100 cm^{-1} that may be assigned to perchlorate being drawn into the optical path as a result of the positive charge.

Turning to the correlation of vibrational and electronic features, Figure 6a shows that carrier I has $\kappa_e > \kappa_D$, suggesting that carrier−carrier interaction is not important. This is consistent with the mean conjugation length being low, so that the average number of carriers per conjugation length is also small. We also expect unkinking/morphological changes to be important. Figure 6b shows a more complicated plot with, apparently, two values of the ratio M_D^0/m_e^0;[44] such behavior may be explained in terms of a change in carrier type. This suggests that carrier I exists *over the full potential range* but carrier II is replaced by a third carrier (denoted carrier III), at potentials $E > 0.7$ V, which is in the region of the point of inflection in the anodic current response in Figure 1c. Furthermore, extrapolating the plot in Figure 6b from the low-potential region (*i.e.*, $E \leq 0.7$ V) shows that it passes through the origin, suggesting that carrier II has charge-independent values of M_D and m_e. However, for $E > 0.7$ V, these parameters become dependent upon the charge (carrier density), with an intercept that suggests morphological changes are important, as for carrier I.

Finally, we seek a structural explanation for the loss of electroactivity upon exposure of the film to very positive

(37) Pham, M.-C.; Aeiyach, S.; Moslih, J.; Soubiran, P.; Lacaze, P. C. *J. Electroanal. Chem. Interfacial Electrochem.* **1990**, *277*, 327.
(38) Christensen, P. A.; Hamnett, A.; Higgins, S. J. *J. Chem. Soc., Dalton Trans.* **1990**, 2233.
(39) Kvarnström, C.; Nybäck, A.-S.; Ivaska, A. *Synth. Met.* **1993**, *55*−57, 503.
(40) Buisson, J. P.; Mevellec, J. Y.; Zeraoui, S.; Lefrant, S. *Synth. Met.* **1991**, *41*−*43*, 287.
(41) Goldenberg, L. M.; Lacaze, P. C. *Synth. Met.* **1993**, *58*, 271.
(42) Pham, M. C.; Moslih, J. *J. Electroanal. Chem. Interfacial Electrochem.* **1991**, *310*, 255.
(43) Pham, M. C.; Moslih, J.; Lacaze, P. C. *J. Electrochem. Soc.* **1991**, *138*, 449.
(44) Christensen, P. A.; Hamnett, A.; Read, D. C. *Synth. Met.* **1994**, *62*, 141.

potentials (E > 1.3 V). In all the polymer spectra, we see a feature at *ca.* 1660 cm^{-1}. This feature is, however, relatively weak when the applied potential is maintained below *ca.* 1.0 V but becomes extremely strong at an applied potential of 1.6 V (compare Figures 3b and S1b). Datta *et al.* report no band in this region for monomeric [Ni(salen)].[24] This feature may be postulated to arise as a consequence of the formation of C═O functionalities, upon overoxidation of the phenyl system, as previously shown upon overoxidation of polypyrrole.[45] In the present case, multiple excursions into the potential region E > 1.3 V result in a steady loss of features attributable to the oxidized form; we were able to avoid these difficulties by restricting the potential range to $E \leq 1.3$ V.

UV−Vis Spectroscopy. The successive transmission spectra, referenced to that of the [Ni(salen)] solution, acquired during the deposition of a [Ni(salen)] film by cycling the working electrode between 0 and 1.3 V (one scan) (Figure S2, Supporting Information) reveal a new band at $\lambda = 490$ nm that starts to appear at $E = 0.85$ V during the positive scan; its intensity increases with cycling until it reaches a maximum at $E = 0.9$V during the negative scan (beginning of the cathodic wave) and then starts to decrease until it reaches roughly 30% of maximum absorbance at the end of the cycle ($E = 0$ V). Spectra acquired by cycling the working electrode between 0 and 1.6 V show the appearance of the band at $\lambda = 490$ nm, the intensity of which increases until $E = 0.8$ V during the negative scan and then starts to decrease until it reaches 50% of maximum absorbance at $E = 0$ V.

The modified electrodes were transferred to a 0.1 mol dm^{-3} TEAP/CH_3CN solution and were cycled once between 0 and 1.0 V at 0.005 V s^{-1} (experimental conditions for reversible redox switching of the film), and electronic spectra were acquired at 0.05 V intervals. The spectrum of the neutral polymer (obtained at 0 V), Figure 7a, is similar to that of the [Ni(salen)] monomer showing one broad low-intensity band at $\lambda = 550$ nm and two poor resolved medium- and high-intensity bands in the range 450−300 nm. As the polymer is oxidized (Figure 7b), the accumulated spectra show an isosbestic point at $\lambda = 370$ nm and the regions at *ca.* 400, 500, and >800 nm show an increase in intensity, whereas the absorbance of the high-energy band at 320 nm decreases.

By depicting the spectra of Figure 7b as differential spectra with reference to that of the neutral polymer, Figure 7c, we can observe that above *ca*. 0.4 V the band at 320 nm decreases in absorbance and that new bands at 410, 456 (sh), and 800 nm (high-energy edge of a band extending out into the near-IR) start to appear. When the potential is raised, at 0.7 V a new band is observed at 540 nm that exhibits a blue shift as the potential is increased. Above 0.95 V, the bands show disparate dependencies with potential: the bands at 410 and 456 nm and in the near-IR (edge) begin to decrease, whereas the band at 320 nm increases; the intensity of the band observed initially at 540 nm continues to increase up to 0.95 V on the negative potential scan but shows $\lambda_{max} = 510$ nm. At the end of the scan, the differential absorbances of these new bands are roughly 2−8% of the maximum differential absorbances observed. Panels a−d of Figure 8 show the differential absorbances of the bands as a function of the potential (first scan); it is clear that the differential absorbances define an almost reversible cycle with very little hysteresis, with the bands at 320 and 410 nm showing similar (but symmetrical) behaviors that are different from that of the band with $\lambda_{max} = 510$ nm.

The band at 456 nm exhibits an Abs *vs* E dependence that is apparently intermediate between these two types of behavior:

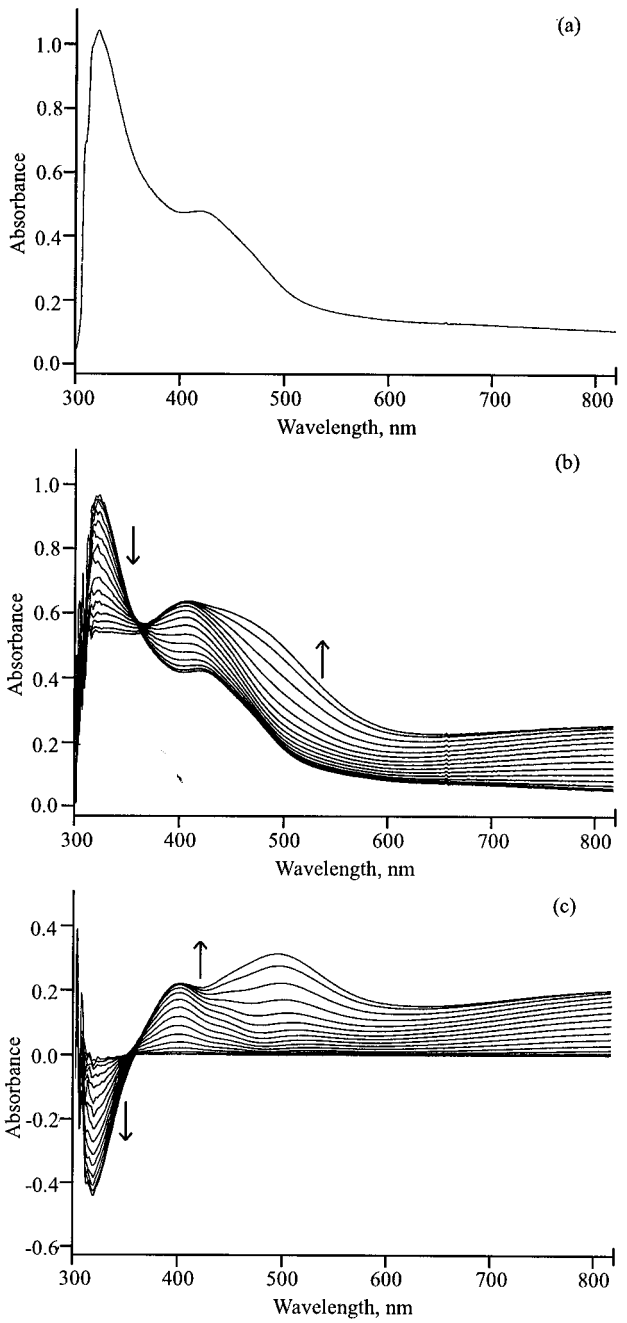

Figure 7. UV−vis transmission spectra of a poly[Ni(salen)]-coated electrode in 0.1 mol dm^{-3} TEAP/CH_3CN: (a) spectrum of the neutral polymer at 0 V, referenced to 0.1 mol dm^{-3} TEAP/CH_3CN; (b) spectra collected from 0 to 1.0 V at 0.05 V intervals and referenced to 0.1 mol dm^{-3} TEAP/CH_3CN; (c) differential spectra of (b) with reference to that of neutral polymer.

it behaves similarly to that with $\lambda = 410$ nm for low polymer oxidation levels but similarly to that with $\lambda_{max} = 510$ nm when the latter band becomes more intense and starts to shift. However, we believe that its Abs *vs* E dependence must be similar to that at 410 nm, since its absorbance for E > 0.8 V is strongly influenced by the high-intensity band at 510 nm.

Differential spectra obtained during subsequent scans exhibit the same electronic features as the spectra acquired during the first scan. After several scans (*ca.* 15 cycles), when a decrease in current intensity is observed, the differential spectra show a reduction in absorbance, but the spectrum of the polymer in the reduced state ($E = 0$ V) is identical to that of the as-grown polymer.

(45) Christensen, P. A.; Hamnett, A. *Electrochim. Acta* **1991**, *36*, 1263.

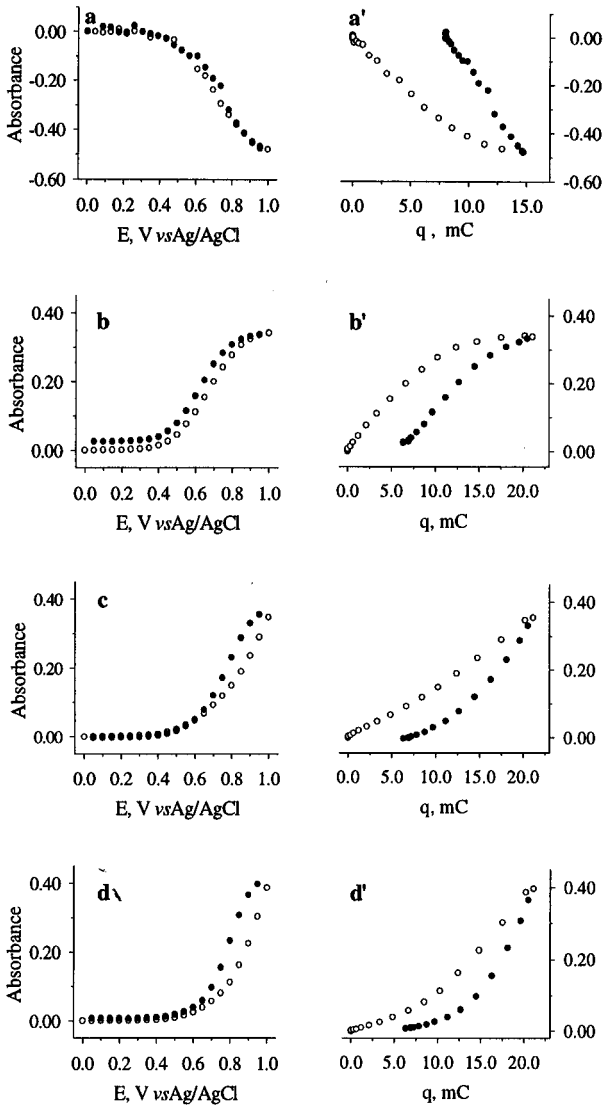

Figure 8. Left: Plots of the differential absorbance of electronic bands *vs E* for λ_{max}: (a) 320, (b) 410, (c) 456, and (d) 510 nm. Right: Plots of then differential absorbance of electronic bands *vs q* for λ_{max}: (a′) 320, (b′) 410, (c′) 456, and (d′) 510 nm. Symbols: ○, positive scan; negative scan.

Taken together, the spectra of the film and the coulometric data from the voltammogram can be used to estimate molar extinction coefficients, $\epsilon(\lambda)/M^{-1}\ cm^{-1}$, by using the expression[46]

$$\mathrm{Abs}(\lambda) = \epsilon(\lambda)\, q/nF \qquad (8)$$

where F is the Faraday constant and q (C cm^{-2}) is the charge density. Panels a′−d′ of Figure 8 show plots of Abs *vs* charge for the electronic bands at 320, 410, 456, and 510 nm. Estimates of the molar extinction coefficients for these electronic bands can be obtained from the slopes of straight-line regions where absorbance change is maximal. Using $n = 0.62$ for the number of electrons transferred per "Ni(salen)" unit, on the basis of coulometric data (see above), the following values are obtained: ϵ(320 nm) ≈ 5600 $M^{-1}\ cm^{-1}$; ϵ(410 nm) ≈ 3400 $M^{-1}\ cm^{-1}$; ϵ(456 nm) ≈ 1600 $M^{-1}\ cm^{-1}$; ϵ(510 nm) ≈ 3200 $M^{-1}\ cm^{-1}$.

A similar study on the oxidation of poly[Ni(salen)], but extending the positive potential limit to 1.6 V, was also undertaken. The main results were as follows: (a) The intensity of the band with initial λ_{max} = 540 nm increases with potential up to 1.40 V, and its energy shifts continuously, ending in a very broad, high-intensity band centered at 480 nm that remains unchanged until 1.1 V on the negative scan and finally starts to decrease. (b) The band at 320 nm decreases until E = 0.9 V on the negative scan, where the absorbance begins to increase. (c) The bands at 410 and 456 nm seem not to increase beyond 0.95 V, but because of the high intensity/large bandwith and λ_{max} proximity of the band at 480 nm, it is difficult to ascertain the real behavior of these bands for high potentials; however, a decrease of the band at 410 nm can be anticipated on the basis of the disappearance of the isosbestic point at 370 nm and the appearance of a new isosbestic point at 405 nm.

As has been pointed out, subsequent scans under these experimental conditions show a substantial decrease in current intensity. The respective differential spectra show the same electronic features as the spectra acquired during the first scan but exhibit greater absolute decrease in the absorbance of all bands. After six scans, when no electrochemical responses are detected, no electronic bands can be observed during the positive cycling of potential. The electronic spectrum of the polymer in the reduced state (E = 0 V), after all these potential cycles, shows, compared to that of the as-grown polymer, a blue shift of the electronic bands in the region 500−350 nm. These observations suggest that all the observed bands in Figure 7c are related to the electroactivity of the polymer and that redox cycling at 1.6 V produces irreversible electronic/structural changes in the polymer.

EPR Experiments. EPR spectra of poly[Ni(salen)] films in the neutral and oxidized states (oxidation at 1.3 and 1.6 V) are presented in Figure 9. Spectral analysis allows for the identification of three independent signals. A sharp signal at g ≈ 2.007 is present in all spectra, both at room temperature and at 77 K, whose intensity is small and independent of the potential (signal I). A small broad component at g = 2.009 is clearly seen only in the spectra at 77 K of the film oxidized at 1.6 V (signal II). Finally, a broad signal (signal III) at g = 2.014 is also observed at both temperatures, although it is more intense at 77 K. The intensity of this component is dependent on the potential, being maximal in the range 1.0−1.3 V.

The EPR spectra observed for poly[Ni(salen)] films are not typical of Ni(III) species[4−7,48] but characteristic of radical species. They exhibit very low g anisotropy and free-electron g features. This contrasts with the large g anisotropy and g_{av} in the range 2.170−2.164 [$g_{av} = {}^1/_3(g_x + g_y + g_z)$] characteristic of electrosynthesized $[Ni^{III}(salen)(DMF)_2]^+$ and $[Ni^{III}(salen)(DMSO)_2]^+$.[7] These results indicate that polymerization of [Ni(salen)] and the oxidative electrochemical properties of the film are not metal-centered but ligand-based processes.

Electronic Characterization of the Polymer in the Neutral and Oxidized States. The absorption spectra of the polymer in the neutral state show bands with λ_{max} values that are similar to those of the monomer, particularly the broad, low-intensity band observed at 550 nm. The latter band is attributed in the monomer to d−d transitions (three unresolved transitions, $d_{xy} \leftarrow \{d_{z^2}; (d_{yz}, d_{xz})$, and $d_{x^2-y^2}\}$[47−49]) and is characteristic of complexes with Ni(II) in a planar tetracoordinate environment, thus suggesting the polymer to have Ni(II) in a planar tetracoordinate sphere similar to that of the metal center in the monomer. The medium- and high-intensity bands of the monomer are assigned respectively to CT and intraligand transitions.[47−49] Due to the similarity between polymer and

(46) Dale, S. M.; Glidle, A.; Hilman, A. R. *J. Mater. Chem.* **1992**, *2*, 99.
(47) Lever, A. B. P. *Inorganic Electronic Spectroscopy*, 2nd ed.; Elsevier: New York, 1984.
(48) Maki, G. *J. Chem. Phys.* **1958**, *28*, 651.
(49) Maki, G. *J. Chem. Phys.* **1958**, *28*, 1129.

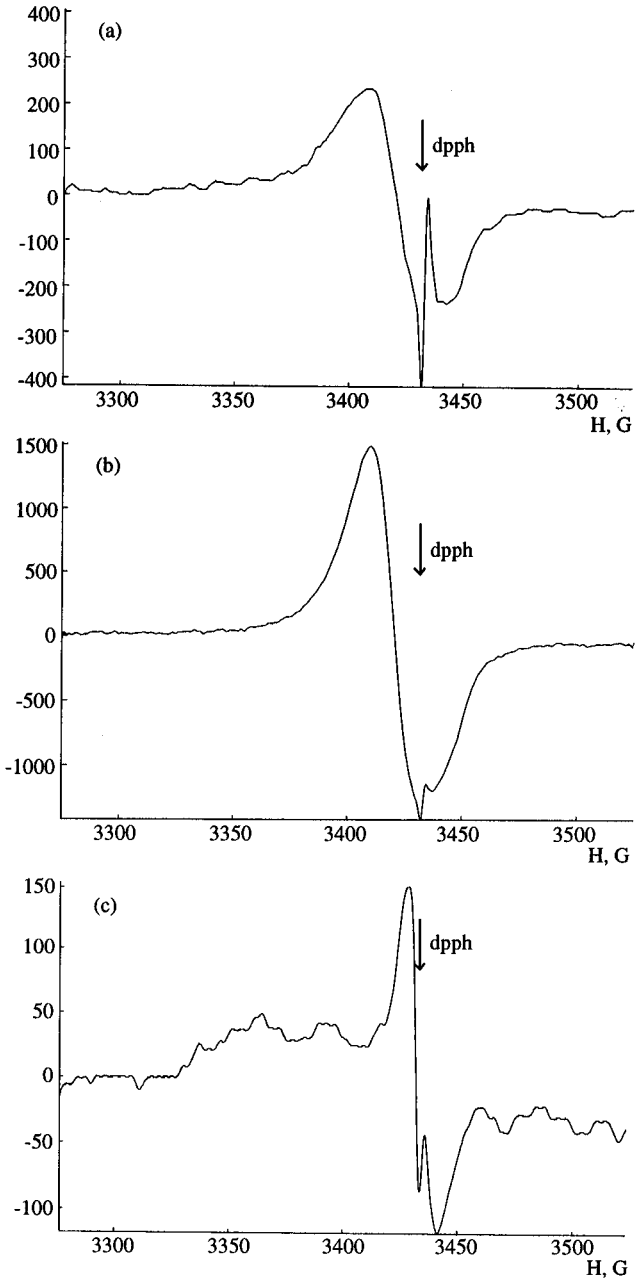

Figure 9. *Ex situ* EPR spectra of poly[Ni(salen)] at 77 K: (a) neutral state, obtained by cycling (10 cycles) the electrode between 0 and 1.3 V with the end of the cycle at 0 V; (b) oxidized state, 1.3 V, obtained by constant-potential electrolysis; (c) oxidized state, 1.6 V, obtained by constant-potential electrolysis. Instrument settings: power, 5 mW; modulation, 100 kHz; sweep center, 3400 G; sweep width, 250 G; sweep time, 336 s.

monomer spectra, the same assignment can be made for these bands of the polymer; any observed small shifts are assumed to arise from new electronic transitions involving ligand-based electronic states that result from monomer condensation.

When the polymer is oxidized, two possible targets for electron release have to be considered: the metal center and the unsaturated ligand. It is known that spectra of monomeric [Ni^{III}(salen)] in DMF and $(CH_3)_2SO$ exhibit two unresolved d−d bands at ≈940 nm ($\epsilon \approx 600\ M^{-1}\ cm^{-1}$), another d−d band at ≈640 nm ($\epsilon \approx 490\ M^{-1}\ cm^{-1}$), and high-intensity CT bands at $\lambda > 600$ nm ($\epsilon > 2000\ M^{-1}\ cm^{-1}$). The intensity of the bands observed during polymer oxidation precludes their assignment to d−d transitions associated with Ni(III) centers; rather, they must be assigned to transitions within states that have a large contribution from the ligand.

At this stage, we note that (a) the bands at 320 and 410 nm have the same Abs *vs E* dependence as the electronic band observed in the FTIR spectra and (b) their absorbance correlates linearly with the intensity of the bands associated with vibration modes involved in the movement of electronic charge along the polymer-chain IRAV bands, for both carrier I and carrier II (Figure S3, Supporting Information). These observations suggest that the electronic bands observed in the UV−visible region must be associated with charge conduction.

Coupling this information with (a) the nonexistence of bands at 410 and 456 nm and 5000 cm^{-1} when the polymer is electroinactive and (b) the radical type EPR spectra exhibited by films in the oxidized state, we further conclude that these electronic bands (a) are due to electronic transitions between states that are generated during polymer oxidation and (b) originate from ligand-based electronic states. Thus we propose to use the polaronic model developed for organic conductors with nondegenerate ground states to interpret our results.[50]

In this model, removal of a single electron from the polymer chain is accompanied by lattice relaxation and generation of a polaron (paramagnetic electronic state). The existence of polaronic states (bonding and antibonding) that lie in the band gap generates three new allowed electronic transitions[33,50] with energies below that of the interband transition. Further removal of electrons leads to generation of more polarons or, if pairing of the charges is energetically favorable and kinetically achievable, to formation of bipolarons. Bipolaronic states in the gap result in only two allowed subgap transitions, since the electronic states are either both occupied or both empty.

We propose the following scheme to interpret/assign the UV−vis spectra of poly[Ni(salen)] in the oxidized state. The electronic bands at 410, 456 nm (3.02, 2.72 eV) and at 800 nm (edge 1.55 eV; maximum intensity at 2040 nm, 0.61 eV), visible at the beginning of polymer oxidation (low doping level), can be assigned to transitions involving states within the band gap. Those at 3.02 and 0.61 eV may be assigned to transitions from the valence band to antibonding and bonding polaron levels and that at 2.72 eV to the transition between the polaron levels.

A check on this assignment is provided by noting that (a) the sum of the lowest energy transitions, $2.72 + 0.61 = 3.33$ eV, is close (within 10%) to that of the high energy, 3.02 eV, and (b) the sum of the energy of the transitions originating in the valence band, $3.02 + 0.61 = 3.63$ eV, is equal to the energy of the band gap, thus implying that it occurs at $\lambda \approx 340$ nm (if a symmetrical location of the gap states is assumed). Additional support for this assignment is provided by noting the decreasing intensity of the band at $\lambda \approx 320$ nm, as expected for an intervalence band. We thus assign the band at 320 nm to the intervalence band.

Before attempting to assign the band at $\lambda_{max} = 510-480$ nm, we will qualitatively analyze our EPR data in the light of the assumptions made above.

The radical associated with signal I (radical I), on the basis of its *g* value and sharpness, can be assigned as a purely organic radical that is able to tumble on the EPR time scale. It is probably associated with terminal radical species of some poly[Ni(salen)] chains, tentatively identified with terminal phenyl groups. Further, as its intensity is independent of the potential and is much smaller than the maximum value of signal III, it is proposed that these radical species must be trapped intermediates from the polymerization process that do not contribute to charge transport.

(50) Bredas, J. In *Handbook of Conducting Polymers*; Skotheim, T. J., Eds.; Marcel Dekker: New York, 1986; Chapter 25.

Signal II (radical II) and signal III (radical III) are weak at 0 V, and as their intensity depends on the potential, we conclude that they must originate from ligand-based oxidation of "Ni(salen)" units in the polymer chain. They are distinguished on the basis of their *g* factors and widths: radical II is a typical organic radical, whereas signal III, due to its high *g* value and large width, must be associated with radical species having a metal contribution to the MO that contains the unpaired spin. In this scheme, radical II appears to be localized on a phenyl ring, whereas radical III is delocalized across phenyl rings and nickel atoms (*via* O−Ni−O or N−Ni−N entities). Therefore, we suggest that radical II is present on polymer chains that are nonlinear, *i.e.* very tangled with no opportunity for extensive π delocalization, whereas radical III exhibits the "normal" behavior seen for conducting polymers.[33,50]

The latter polarons must reside on linear sections of the polymer long enough to accommodate more than one polaron, and chain linearity allows them to be mobile through nickel centers. At more positive potentials, their concentration is high, and pairing to form bipolarons (diamagnetic states) becomes energetically favorable. Support for polaron pairing to form bipolarons is provided by the observed maximum in the intensity of the EPR signal in the range 1.0−1.3 V.[51] For radical II, delocalization is not extensive enough to accommodate more than one positive charge, and since movement of charge around a "corner" of a chain is difficult, these polarons are not able to pair up to form bipolarons. This would account for the observation of radical II at very positive potentials, where we would normally expect them to have been replaced by bipolarons.

In the context of the above discussion, the electronic band that starts to increase at 0.7 V and shows an absorbance maximum between 1.4 V in the positive scan and 1.1 V in the negative scan (λ_{max} = 480 nm) may be due to the presence of bipolarons. The electronic spectra acquired during polymer redox cycling in the range 0−1.6 V provide further proof for the assumption of polaron pairing: the absorbance of the band at 410 nm (associated with polaron transitions) decreases and reaches a local minimum in the potential range for which the band at 480 nm is more intense. Thus we assign the latter electronic band to the transition valence band → antibonding bipolaron level.

Correlating all the spectroscopic data allows us to propose that carrier I and carrier II, identified from FTIR results, are polarons associated with signal II and signal III, respectively, in the EPR spectra and are responsible for the electronic bands at 3.02, 2.72, and 0.61 eV.

Furthermore, structural information and charge conducting properties of both carrier I and II obtained from FTIR spectroscopy are also consistent with EPR data: (a) carrier I is associated with IRAV bands that are mainly due to phenyl vibration modes and exhibits carrier−carrier interactions that suggest a low mean conjugation length and a small average number of carriers per conjugation length; (b) carrier II is associated with IRAV bands that include vibrations of O−Ni−O modes and shows charge-independent values of M_D and m_e for $E < 0.7$ V. For higher potential values, the latter parameters become dependent upon the charge, where carrier II is replaced by a third carrier, denoted as carrier III, that we tentatively assigned as a bipolaron on the basis of EPR and electronic data.

Concluding Remarks

Our study confirms the limitations of the use of electrochemical techniques *per se* to fully characterize electrogenerated polymers, and we stress the need to combine several other techniques, *viz*. spectroscopic, to achieve such a characterization.

In fact, a combination of electrochemical *and* spectroscopic techniques has revealed that electropolymerization of [Ni(salen)] is ultimately a ligand-based-process that probably takes place through a mixture of *o*- and *p*-linking of the phenyl ring. Also, poly[Ni(salen)], although based on a *bona fide* coordination compound, exhibits physical/chemical properties that cannot be attributed to an aggregation of individual complexes (redox polymer). Rather, it behaves like a polyphenylene compound, with the metal ion acting as a bridge between biphenylene moieties, analogous to a conducting organic polymer. The main charge carriers involved in the conduction process under moderate conditions were identified as paramagnetic radicals associated with polaron states in the band gap. At higher levels of doping, removal of a second charge led to the formation of a diamagnetic dication (bipolaron) through pairing of cation radicals.

To obtain a full understanding of the electronic structure and conducting properties of these materials, it is important to extend these studies to polymers based on metal complexes with salen-based ligands that will exhibit reversible electroactivity in a wider potential window.

Acknowledgment. This work was partially supported by the JNICT through Project PBIC/QUI/2137/95. M.V.-B. thanks the JNICT/Praxis XXI for a fellowship.

Supporting Information Available: A table of IR absorptions of the monomer and neutral polymer and figures showing polymer FTIR spectra normalized to the spectrum of the coated electrode at 0.3 V, electronic spectra acquired during the polymerization, and a plot of differential absorbance of the electronic bands (λ_{max} = 320, 410, 456, 510 nm) *vs* intensity of IRAV bands (4 pages). Ordering information is given on any current masthead page.

IC970467J

(51) Bandley, H. L.; Cremins, P.; Garner, S. E.; Hillman, A. R.; Raynor, J. B.; Workman, A. D. *J. Electrochem. Soc.* **1995**, *142*, 2111.